The synergistic effect of Na$_3$PO$_4$ and benzotriazole on the inhibition of copper corrosion in tetra-*n*-butylammonium bromide aerated aqueous solution

S. Liu*, J. Dong, W. W. Guan, J. M. Duan, R. Y. Jiang, Z. P. Feng and W. J. Song

The effect of Na$_3$PO$_4$ and the mixture of benzotriazole (BTA) and Na$_3$PO$_4$ (SP) on the corrosion of copper in 17 wt% (0.534 mol/L) tetra-*n*-butylammonium bromide (TBAB) aerated aqueous solution has been investigated by means of weight-loss test, potentiodynamic polarization test, electrochemical impedance spectroscopy (EIS), and scanning electron microscopy/energy dispersive X-ray techniques. The experimental results showed that a dosage of Na$_3$PO$_4$ stimulated the copper corrosion, and the corrosion rate increased with increasing Na$_3$PO$_4$ concentration, whereas the mixture of BTA and Na$_3$PO$_4$ could protect copper in aqueous TBAB solution. The inhibition action of the mixture of BTA and Na$_3$PO$_4$ on the corrosion of copper is mainly due to the inhibition of the anodic process of corrosion. The inhibition efficiency of a mixture consisting of 2 g/L BTA and 1 g/L Na$_3$PO$_4$ was about 96%. The mixture of BTA and Na$_3$PO$_4$ inhibits the corrosion of copper better than BTA by itself, indicating that Na$_3$PO$_4$ has a synergistic role with BTA on the corrosion inhibition of copper in TBAB aqueous solution.

1 Introduction

The clathrate hydrate crystal of tetra-*n*-butylammonium bromide (TBAB) has advantages as cold-storage material over ice in the air-conditioning system because it has higher phase-change temperature (0–12 °C) and can be transported directly through pipelines [1, 2]. The phase diagram, latent heat, specific heat, structure, free-growth forms, growth kinetics, and growth mechanism of TBAB clathrate hydrate crystals have been studied by many scientists [1–5], but there were very few investigations concerning the corrosion behavior of metals used to make the pipelines, valves, and heat exchangers of air-conditioning system in aqueous TBAB solution containing aggressive bromide anions [6–8].

One way of protecting metals from corrosion is to use corrosion inhibitors. The remarkable efficiency of benzotriazole (BTA) as corrosion inhibitor of copper has been well established and the protective action of BTA has been attributed to the formation of a protective film of Cu (I) BTA or an adsorbed layer of BTA on the copper surface [9–32]. The published literature about the effect of orthophosphate on the copper corrosion is contradictory [33–42]. In some cases, a dosage of orthophosphate inhibited the copper corrosion through the formation of a protective cupric phosphate or similar scale on the copper surface [33–42]; however, in some cases phosphate stimulated the copper corrosion by hindering the formation of a protective malachite layer [38–42].

In previous papers [6–8], we studied the corrosion inhibition of carbon steel and zinc in TBAB aerated aqueous solution by BTA and Na$_3$PO$_4$ (SP) and the corrosion inhibition of copper by BTA, and found that both of them could effectively inhibit the corrosion of carbon steel and zinc and BTA could effectively inhibit the corrosion of copper. For carbon steel and zinc, the inhibitor combinations led to higher efficiencies compared to those obtained when added individually. In the present paper, based on our previous research results, we investigated the action of Na$_3$PO$_4$ and the mixture of BTA and Na$_3$PO$_4$ as copper corrosion inhibitor in 17 wt% (0.534 mol/L) TBAB aerated aqueous solution by weight-loss test, open circuit potential (OCP) test, potentiodynamic polarization test, electrochemical impedance spectroscopy (EIS), and scanning electron microscopy (SEM)/energy dispersive X-ray spectroscopy (EDX) techniques.

S. Liu, J. Dong, W. W. Guan, J. M. Duan, R. Y. Jiang
Department of Applied Chemistry, South China University of Technology, Guangzhou 510640 (P. R. China)
E-mail: chsliu@scut.edu.cn

Z. P. Feng, W. J. Song
Guangzhou Institute of Energy Conversion, CAS, Guangzhou 510640 (P. R. China)

2 Experimental

Specimens used were electrolytic Cu (99.99%). Prior to the measurements, the exposed surface was ground with emery papers (grade 200-1200) and then rinsed with double distilled water and finally dried. The electrolytes were prepared using analytical chemicals and distilled water.

Weight-loss experiments were performed using specimens of dimensions $50\,mm \times 25\,mm \times 2\,mm$ in triplicate. The tests were conducted for 240 days by placing them into the test solution. After the stipulated time period, samples were taken out rinsed with distilled water, dried, and weighed.

Electrochemical measurements were performed in three-electrode glass cell at room temperature, a platinum electrode was used as counter electrode, and saturated calomel electrode (SCE) was used as reference electrode. The working electrode in this work was embedded in epoxy resin, leaving a geometrical surface area of $0.5\,cm^2$ exposed to the electrolyte. Potentiodynamic (Tafel) polarization curves and electrochemical impedance measurements were carried out using a computer controlled CHI 660C Electrochemical Workstation, accordingly all experiments were carried out after 0.5 h immersion of the metal specimens into the electrolyte.

Tafel polarization curves were obtained using a sweep rate of 0.5 mV/s in the potential range of $\pm 200\,mV$ with respect to the initial OCP. The linear Tafel segments of the anodic and cathodic curves were extrapolated to corrosion potential to obtain the corrosion current densities.

Electrochemical impedance spectra were obtained in the frequency range of 100 kHz–0.01 Hz with perturbation amplitude of 5 mV at the corrosion potential.

Examination of copper surface after 5 days exposure to the 17 wt% TBAB solution without and with BTA was performed by LEO1530VP Scanning Electron Microscope. Rough elemental analyses for the exposed surface were conducted by EDX technique.

3 Results

3.1 Weight-loss measurements

Table 1 shows the corrosion rate and inhibition efficiency (IE) of copper obtained by weight-loss measurements for different concentrations of Na$_3$PO$_4$, BTA, and their mixture. The corrosion IE was calculated as follows [28, 29]:

$$IE(\%) = \frac{W_0 - W}{W_0} \times 100 \qquad (1)$$

where W_0 and W are the values of weight-loss of copper after 240 days of immersion in solutions in the absence and presence of inhibitor(s), respectively.

As indicated in Table 1, a dosage of Na$_3$PO$_4$ stimulated the copper corrosion, and the corrosion rate increased with increasing Na$_3$PO$_4$ concentration. It is clear that the addition of the mixture of BTA and Na$_3$PO$_4$ decreases the value of corrosion rate. The mixture inhibits the corrosion of copper better than BTA by itself, indicating that Na$_3$PO$_4$ has a synergistic role

Table 1. Corrosion rate of copper and IE of BTA, Na$_3$PO$_4$, and their mixture for the corrosion of copper in 17 wt% TBAB solution obtained from weight-loss measurements

C_{BTA} (g/L)	C_{SP} (g/L)	pH	Corrosion rate (mg/m^2/h)	IE (%)
0	0	6.0	1.31	–
0.1	0	5.7	1.032	21.2
0.5	0	5.4	0.303	76.9
1	0	5.3	0.197	85.0
2	0	5.1	0.131	90.0
4	0	5.0	0.086	93.4
6	0	4.9	0.076	94.2
0	0.1	10.9	3.11	–
0	0.5	11.5	6.72	–
0	1	11.8	10.3	–
0	2	11.9	13.9	–
0	4	12.0	17.0	–
0	6	12.1	18.5	–
0.01	0.01	9.9	0.822	37.2
0.01	0.05	10.6	0.532	59.4
0.01	0.5	11.5	0.425	67.6
0.01	2	11.9	0.382	70.8
0.05	0.05	10.6	0.132	89.9
0.05	0.5	11.5	0.093	92.9
0.05	1	11.8	0.116	91.1
0.05	2	11.9	0.122	90.7
0.1	0.05	10.6	0.098	92.5
0.1	0.1	10.9	0.086	93.4
0.1	0.5	11.5	0.106	91.9
0.1	2	11.9	0.113	91.4
0.5	0.1	10.9	0.070	94.7
0.5	0.5	11.5	0.077	94.1
0.5	1	11.8	0.082	93.7
0.5	2	11.9	0.094	92.8
2	0.5	11.5	0.0502	96.2
2	1	11.8	0.0487	96.3
2	2	11.9	0.0496	96.2
2	4	12.0	0.0534	95.9

with BTA on the corrosion inhibition of copper in TBAB aqueous solution (in this study, synergy is defined as a combination of inhibitors that produces a lower amount of measured corrosion than the single best chemical constituent [43]). For example, the corrosion rate of copper was 0.131 mg/m^2/h in presence of 2 g/L BTA, however, the corrosion rate decreased greatly to 0.0487 mg/m^2/h in presence of the mixture of 2 g/L BTA and 1 g/L Na$_3$PO$_4$.

3.2 Potentiodynamic (Tafel) polarization measurement

The obtained Tafel polarization curves for copper without and with inhibitor(s) are shown in Fig. 1. Table 2 indicates the Tafel polarization parameters for electrolyte without and with inhibitor(s), such as the corrosion potential (E_{corr}), the corrosion current density (I_{corr}), cathodic and anodic Tafel slopes (b_c and b_a), and IE. The IE of the inhibitor has been calculated using [24]:

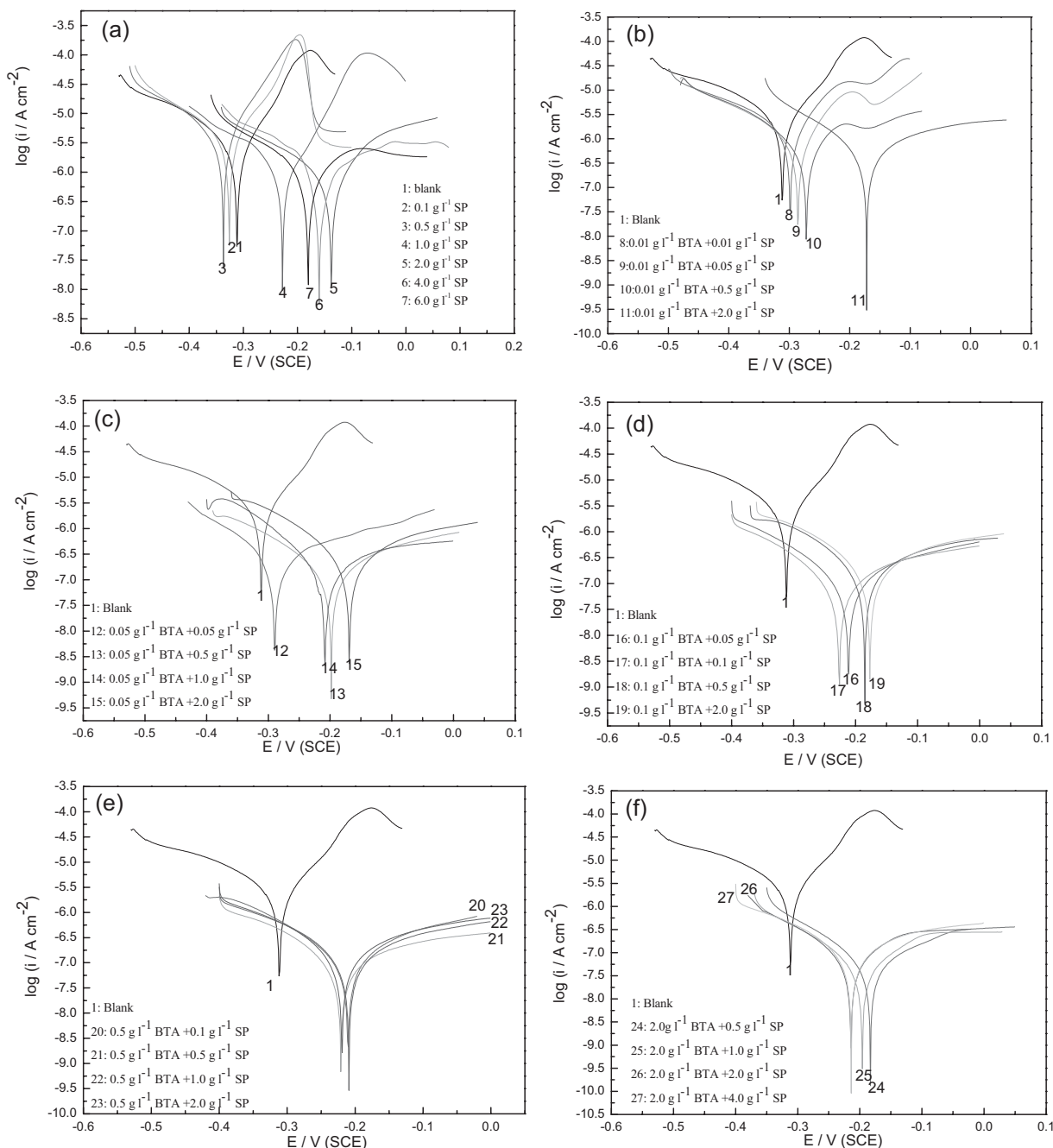$$IE\% = \frac{I_{corr}^0 - I_{corr}}{I_{corr}^0} \times 100 \qquad (2)$$

Figure 1. Potentiodynamic polarization curves for copper in 17 wt% TBAB solution containing the mixture in the presence of the following concentrations of BTA (g/L): (a) 0, (b) 0.01, (c) 0.05, (d) 0.1, (e) 0.5, (f) 2. The number in Fig. 1 is identical to that in Table 2

where I_{corr}^0 and I_{corr} are the corrosion current density of copper in solutions without and with inhibitor(s), respectively.

As indicated in Table 2 and Fig. 1, in the presence of Na₃PO₄ only, low (0.1–0.5 g/L) doses of Na₃PO₄ stimulated the copper corrosion (increase of the corrosion current density), whereas high (1–6 g/L) doses of Na₃PO₄ inhibited the copper corrosion (decrease of the corrosion current density). When the mixture of BTA and Na₃PO₄ was added to 17 wt% TBAB aqueous solution, a reduction of the corrosion current density (I_{corr}) and anodic current density was observed, together with a shift of E_{corr} in the

anodic direction (Fig. 1 and Table 2). Based on the marked decrease of the anodic current density and the positive shift in the corrosion potential upon introduction of the mixture in the aggressive solution, the mixture of BTA and Na₃PO₄ is considered as inhibitor of predominant anodic effect [44].

3.3 Impedance spectroscopy

Impedance data in the form of Nyquist plots of copper at the OCP in 17 wt% TBAB without and with inhibitor(s) are presented in

Table 2. Polarization parameters of Na_3PO_4 and the mixture of BTA and Na_3PO_4 in 17 wt% TBAB solution

No.[a]	C_{BTA} (g/L)	C_{SP} (g/L)	E_{corr} (mV (SCE))	I_{corr} ($\mu A/cm^2$)	b_a (mV/dec)	b_c (mV/dec)	IE (%)
1	0	0	312	3.220	81.21	181.0	–
2	0	0.1	345	4.800	81.86	195.5	–
3	0	0.5	327	4.060	74.44	182.5	–
4	0	1	228	1.790	82.13	237.0	44.4
5	0	2	147	0.887	128.4	203.8	72.5
6	0	4	157	1.030	332.2	184.2	68.0
7	0	6	174	1.230	218.3	177.9	61.8
8	0.01	0.01	298	1.870	95.36	201.6	41.9
9	0.01	0.05	284	1.050	82.86	165.2	67.4
10	0.01	0.5	273	0.778	150.2	143.5	75.8
11	0.01	2	170	0.582	241.5	141.8	81.9
12	0.05	0.05	290	0.299	247.2	147.9	90.7
13	0.05	0.5	198	0.155	222.1	150.8	95.2
14	0.05	1	208	0.177	288.7	112.9	94.5
15	0.05	2	170	0.255	224.3	130.2	92.1
16	0.1	0.05	212	0.128	258.1	150.5	96.0
17	0.1	0.1	227	0.108	251.3	146.5	96.6
18	0.1	0.5	185	0.190	262.0	141.4	94.1
19	0.1	2	178	0.206	252.7	145.4	93.5
20	0.5	0.1	209	0.137	252.0	157.3	95.7
21	0.5	0.5	221	0.104	304.0	146.0	96.8
22	0.5	1	212	0.143	207.6	144.5	95.6
23	0.5	2	219	0.155	240.7	153.0	95.2
24	2	0.5	182	0.059	189.8	127.7	98.2
25	2	1	196	0.056	154.7	130.8	98.3
26	2	2	214	0.082	178.3	136.6	97.5
27	2	4	216	0.107	261.5	160.8	96.7

[a]The number in Table 2 is identical to that in Figs. 1 and 2.

Fig. 2. The complex plane spectra exhibit a depressed semicircle with the center under the real axis, and such behavior is characteristic for solid electrodes and is often referred to as frequency dispersion and attributed to the roughness and other inhomogeneities of the solid electrode. A diffusion tail at low frequencies suggested the presence of Warburg impedance [16]. The Warburg impedance observed can be attributed to the diffusion of soluble copper species from the electrode surface to the bulk solution or the diffusion of dissolved oxygen or aggressive anions (Br^-) from the bulk solution to the electrode surface.

An equivalent circuit [6–8] shown in Fig. 3 was used to fit the impedance data obtained from the 17 wt% TBAB aqueous solution in the absence and presence of inhibitor(s). In this figure, R_e represents the solution resistance, R_{ct} the charge transfer resistance, R_f the resistance of the film formed; W is the Warburg impedance element, for which a lower value indicates a greater resistance of the diffusion of corrosive agents [45]. $Q1$ represents the capacitive behavior at the electrolyte/metal interface (i.e., the double layer), $Q2$ the capacitive behavior of the passive film formed. The symbols Q signify the possibility of a non-ideal capacitance (CPE, constant phase element) with varying n. The appearance of the CPE element is often related to the electrode roughness or to the inhomogeneity in the conductance or dielectric constant [20, 26]. The impedance of the CPE is given

by [16, 20, 26]:

$$Q = Z_{CPE}(\omega) = [Cj\omega^n]^{-1} \tag{3}$$

For $n = 1$, the Q element reduces to a capacitor; for $n = 0$, to a simple resistor and for $n = 0.5$, to a Warburg impedance element.

The points in Fig. 2 represent experimental data and the solid lines are spectra simulations based on the proposed electrical equivalent circuit shown in Fig. 3. The fitted parameters are summarized in Table 3.

The IE of the inhibitor has been calculated using [6–8, 28]:

$$IE\% = \frac{R_{ct} - R_{ct}^0}{R_{ct}} \times 100 \tag{4}$$

where R_{ct}^0 and R_{ct} are charge transfer resistance for copper in 17 wt%TBAB in the absence and presence of inhibitor(s), respectively.

As shown in Table 3, in the presence of Na_3PO_4 only, low (0.1–0.5 g/L) doses of Na_3PO_4 stimulated the copper corrosion (decrease in charge transfer resistance), whereas high (1–6 g/L) doses of Na_3PO_4 inhibited the copper corrosion (increase of the corrosion current density). The addition of the mixture of BTA and Na_3PO_4 caused an increase in charge transfer resistance (R_{ct}), a decrease in the capacitance of the double layer ($Q1$) and a
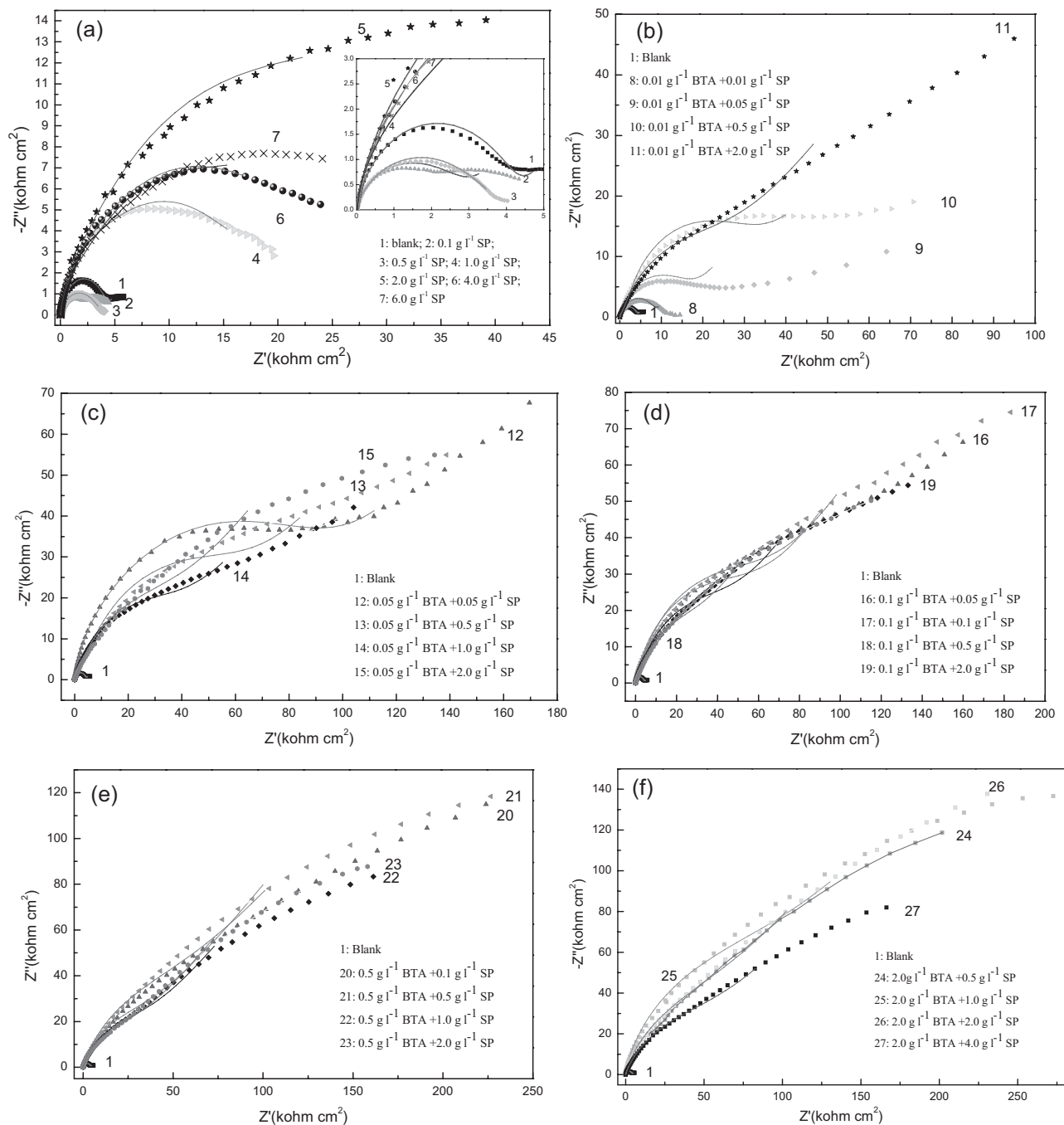
Figure 2. Nyquist plots for copper in 17 wt% TBAB solution containing the mixture in the presence of the following concentrations of BTA (g/L): (a) 0, (b) 0.01, (c) 0.05, (d) 0.1, (e) 0.5, (f) 2. The number in Fig. 2 is identical to that in Table 2. The points represent experimental data and the solid lines are spectra simulations based on the proposed electrical equivalent circuit shown in Fig. 3

decrease of Warburg impedance element (W). These results indicate that the mixture of BTA and Na$_3$PO$_4$ is an efficient copper corrosion inhibitor in TBAB solution. The magnitude of the double layer capacitance ($Q1$) was reduced on addition of the mixture of BTA and Na$_3$PO$_4$ to the solution, which can be attributed to the formation of the protective cupric phosphate or similar scale and adsorption of BTA on the copper surface.

As it is observed in Tables 1–3, the corrosion IEs (or trends) determined by the three methods (weight-loss test, Tafel polarization, and impedance measurement) are in reasonably good agreement for the mixture of BTA and Na$_3$PO$_4$, but in disagreement for Na$_3$PO$_4$.

3.4 Surface analysis

The highly corroded surface of the copper panel after 5 days of immersion in a solution of 17 wt% TBAB without inhibitor was observed by SEM (Fig. 4a), and EDX analysis showed the presence
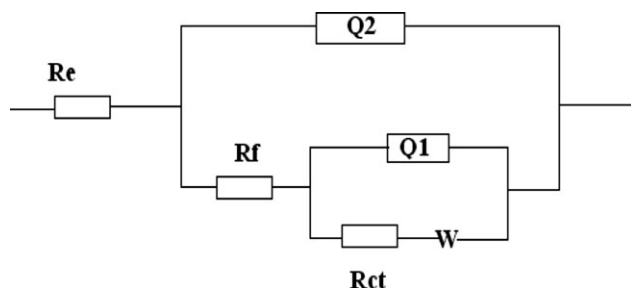
Figure 3. Equivalent circuit used to fit the EIS data on copper surface in 17 wt% TBAB solution without and with inhibitor(s)

of Cu and Br (Fig. 4b) in the corrosion products composition. In the presence of BTA (4 g/L), the copper surface had an almost clean appearance with some deposits of corrosion products (Fig. 5a), and the reduced intensity of bromine peak of EDX spectrum (Fig. 5b) is due to the decrease of CuBr (one of the corrosion products) [46]. In the presence of Na_3PO_4 (2 g/L), a more severely corroded surface was observed compared with that in the blank solution (Fig. 6a) and EDX analysis showed also the presence of Cu and Br (Fig. 6b) in the corrosion products composition, indicating that Na_3PO_4 stimulated the copper corrosion. The SEM image of the surface of a panel formed in the presence of a mixture in proportion of 2 g/L BTA and 1 g/L Na_3PO_4 is shown in Fig. 7a. The surface still showing clear polishing lines was almost free from corrosion, and the reduced intensity of bromine peak of EDX spectrum (Fig. 7b) is

due to the decrease of CuBr (one of the corrosion products) [46] and the EDX spectrum showed a trace of P and N which could be attributed to the presence of cupric phosphate and BTA molecules on the copper surface.

4 Discussion

In some cases, a dosage of orthophosphate inhibited the copper corrosion, due to the formation of a protective cupric phosphate or similar scale on the copper surface [33–42]. On the other hand, in some cases phosphate stimulated the copper corrosion, since phosphate hindered the formation of a protective malachite layer [39–42]. The results of potentiodynamic polarization test and electrochemical impedance test (Tables 2 and 3) showed that high (1–6 g/L) doses of Na_3PO_4 inhibited the copper corrosion. However, from the results of weight-loss test and surface analysis (Table 1 and Fig. 6), we noted a significant acceleration of the copper corrosion process after the addition of Na_3PO_4 in 17% TBAB electrolyte. The weight-loss test evaluates the corrosion rate as an average value over the exposure period, i.e., is a long-term test. In contrast, the potentiodynamic polarization test and electrochemical impedance test are essentially instantaneous techniques which provide a measurement of corrosion rate at a particular time over which the measurement was carried out [47, 48], i.e., are short-term tests. The results of long-term test are more reliable [49]. Therefore, a conclusion was drawn that Na_3PO_4 stimulated the copper corrosion in 17% TBAB

Table 3. Impedance parameters during corrosion inhibition of copper in 17 wt% TBAB solution with and without inhibitor(s)

C_{BTA} (g/L)	C_{SP} (g/L)	$Q1 \times 10^6$ ($\Omega^{-1} s^n/cm^2$)	$Q2 \times 10^6$ ($\Omega^{-1} s^n/cm^2$)	n_1	n_2	R_f ($\Omega\,cm^2$)	R_{ct} ($k\Omega\,cm^2$)	$W \times 10^4$ ($\Omega^{-1} s^{0.5}/cm^2$)	IE (%)
0	0	48.26	35.98	0.78	0.95	13.68	4.170	48.10	–
0	0.1	144.4	39.00	0.55	0.97	7.245	3.083	56.40	–
0	0.5	164.3	37.70	0.54	0.97	11.60	3.720	385.2	–
0	1	201.8	63.40	0.74	0.9	7305	9.320	21.02	55.3
0	2	123.6	77.00	0.74	0.9	7475	21.08	4.854	80.2
0	4	160.6	86.90	0.65	0.9	5935	16.39	18.30	74.6
0	6	178.4	76.70	0.74	0.93	4423	13.53	8.254	69.2
0.01	0.01	55.12	1.693	0.78	0.95	7.510	8.430	22.56	50.5
0.01	0.05	24.84	9.110	0.74	0.93	10.64	17.20	4.072	75.7
0.01	0.5	26.68	21.94	0.98	0.90	7110	24.57	2.212	83.6
0.01	2	21.78	4.058	0.74	0.97	1197	28.61	1.058	85.4
0.05	0.05	1.399	7.294	0.75	0.90	47580	50.85	0.913	91.8
0.05	0.5	13.76	4.898	0.80	0.93	8100	57.45	0.881	92.7
0.05	1	21.98	4.354	0.74	0.97	492.8	43.83	1.198	90.5
0.05	2	17.31	5.476	0.74	0.90	1789	42.24	0.744	90.1
0.1	0.05	9.144	2.142	0.74	0.97	18.60	62.35	0.663	93.3
0.1	0.1	9.196	3.210	0.73	0.97	4534	65.05	0.611	93.6
0.1	0.5	14.56	5.060	0.74	0.93	3414	47.91	0.802	91.3
0.1	2	21.78	7.110	0.74	0.88	1044	36.10	0.886	88.4
0.5	0.1	8.262	2.142	0.80	0.97	12.95	39.87	0.357	89.5
0.5	0.5	12.81	6.994	0.74	0.93	3357	67.15	0.386	93.8
0.5	1	11.72	6.548	0.74	0.93	2552	36.81	0.548	88.7
0.5	2	10.46	6.250	0.74	0.93	2013	31.64	0.498	86.8
2	0.5	14.56	8.439	0.68	0.97	50.43	80.45	0.440	95.1
2	1	13.03	5.650	0.77	0.98	18.78	114.3	0.362	96.4
2	2	16.94	2.948	0.74	0.97	10.36	79.50	0.371	94.8
2	4	18.79	2.656	0.65	0.97	19.86	78.50	0.607	94.7

(a)

(a)

(b)

(b)

Figure 4. SEM image (a) and EDX spectrum (b) of copper immersed for 5 days in 17 wt% TBAB aqueous solution
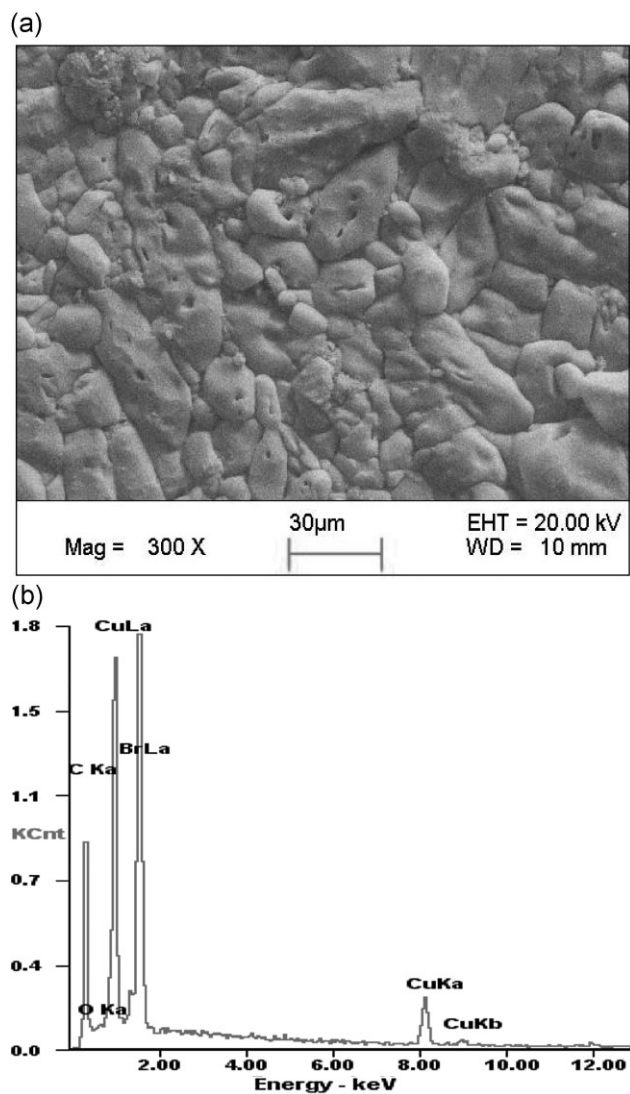
Figure 5. SEM image (a) and EDX spectrum (b) of copper immersed for 5 days in 17 wt% TBAB aqueous solution with 4 g/L BTA

aqueous solution. When the immersion time of copper into the electrolyte was short (0.5 h in this study), high (1–6 g/L) doses of Na₃PO₄ probably led to the formation of a protective cupric phosphate or similar scale [39–42], but for the electrolyte without Na₃PO₄ within the short time the effectively protective malachite layer probably had not been formed yet. So the results of the potentiodynamic polarization test and electrochemical impedance test (Tables 2 and 3) showed that high (1–6 g/L) doses of Na₃PO₄ inhibited the copper corrosion. When the immersion time was relatively longer (not shorter than 5 days), a dosage of Na₃PO₄ hindered the formation of malachite, therefore the results of weight-loss and surface analysis showed that Na₃PO₄ stimulated the copper corrosion in 17% TBAB aqueous solution.

It is well-known that the inhibitive action of organic compounds containing N is due to the formation of co-ordinate type bond between the metal and the lone pair of electrons of the additive. BTA is described as a good inhibitor for copper. The protective action of BTA has been attributed to the formation of a
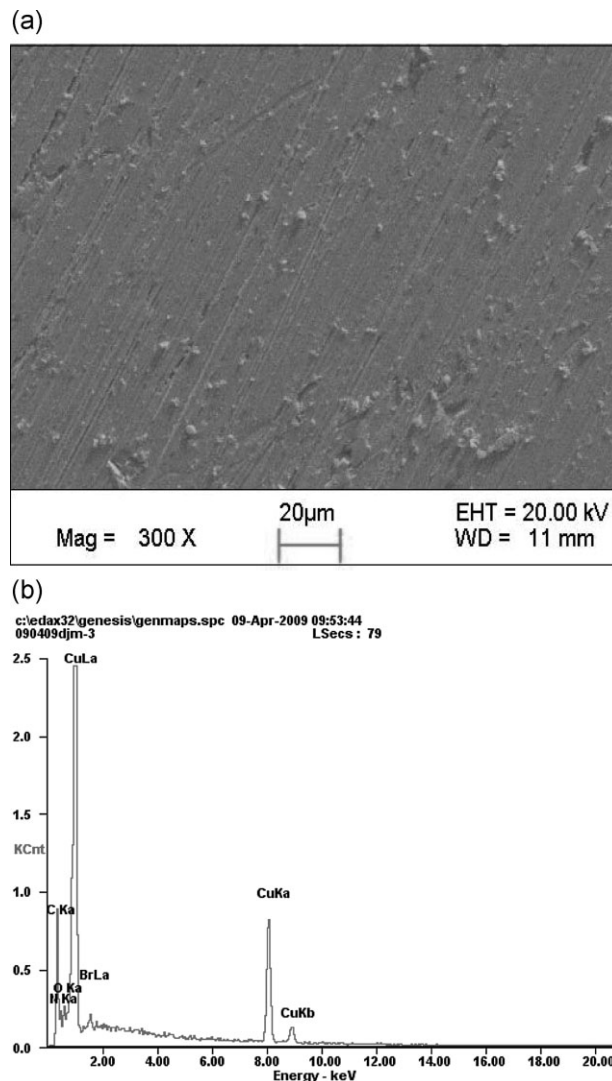
protective film of Cu (I) BTA or an adsorbed layer of BTA on the copper surface [9–32]. As indicated in Table 1, the mixture of BTA and Na₃PO₄ exhibited a higher protection efficiency against the corrosion of copper in 17% TBAB aqueous solution than BTA alone. In previous papers [6, 7], we have also found the inhibitor combinations resulted in higher efficiencies in the corrosion inhibition of carbon steel and zinc compared to those obtained when added individually for the TBAB solution. We inferred that the main function of Na₃PO₄ seemed to form the layer containing Fe phosphate and γ-Fe₂O₃ for carbon steel or ZnO, Zn(OH)₂, and Zn₃(PO₄)₂ for zinc, whereas BTA could stabilize this layer by incorporation into it or/and adsorption on it. *Rammelt* et al. [50] have investigated the synergistic effect of benzoate and BTA on passivation of mild steel in near neutral air saturated aqueous solution. They think benzoate acts primarily on the rate of iron dissolution by plugging the pores in the air formed oxide layer with insoluble ferric benzoate complexes, whereas BTA is strongly adsorbed on the oxide layer. The synergistic effect in
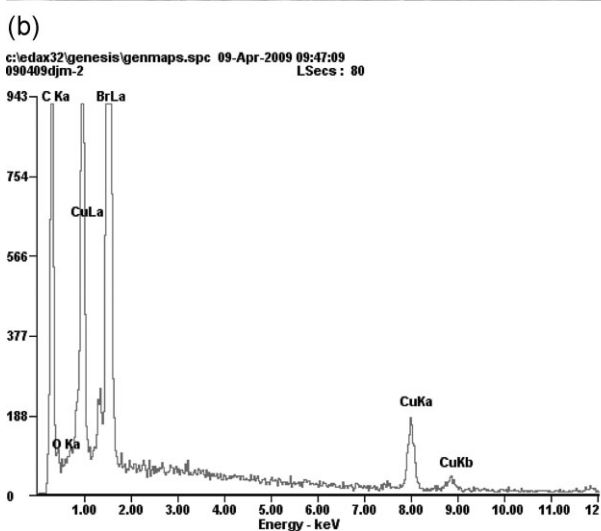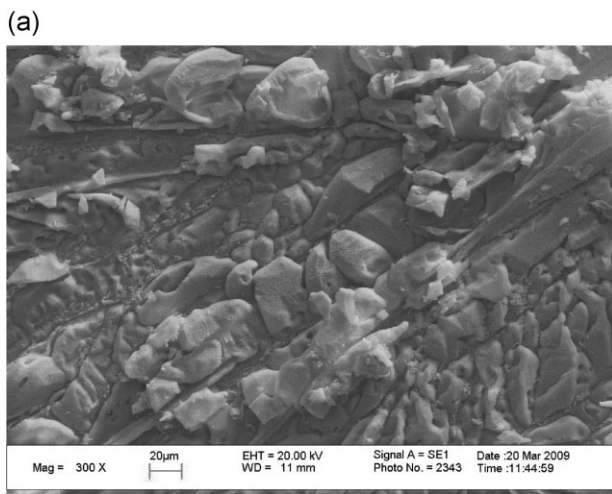
(a)

(b)

Figure 6. SEM image (a) and EDX spectrum (b) of copper immersed for 5 days in 17 wt% TBAB aqueous solution containing 2 g/L Na_3PO_4

(a)

(b)

Figure 7. SEM image (a) and EDX spectrum (b) of copper immersed for 5 days in 17 wt% TBAB aqueous solution in the presence of a mixture in proportion of 2 g/L BTA and 1 g/L Na_3PO_4

the corrosion is due to a more favorable adsorption of BTA compared with benzoate. Insofar that the conclusions of the cited investigation [50] can be transposed to the present case of BTA and Na_3PO_4 on copper, this finding implies that the main function of Na_3PO_4 is to form the cupric phosphate or similar scale, whereas BTA can stabilize this scale by incorporation into it or/and adsorption on it conjectured by the N and P signals of EDX spectrum (Fig. 7b) so that corrosion inhibition occurs after immersion of copper into the solution containing the mixture of BTA and Na_3PO_4. A synergistic effect in the corrosion can mainly be attributed to the formation of the scale by Na_3PO_4 and strong adsorption of BTA on the scale or/and incorporation of BTA into the scale.

5 Conclusions

The action of Na_3PO_4 and the mixture of BTA and Na_3PO_4 as copper corrosion inhibitor in 17 wt% (0.534 mol/L) TBAB aerated aqueous solution has been investigated by weight-loss tests, Tafel
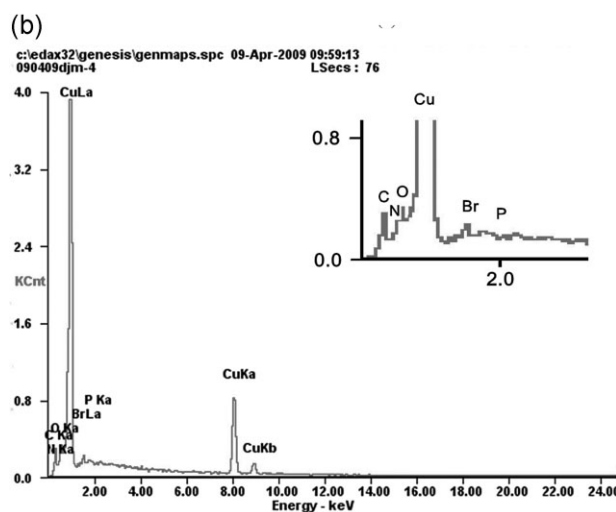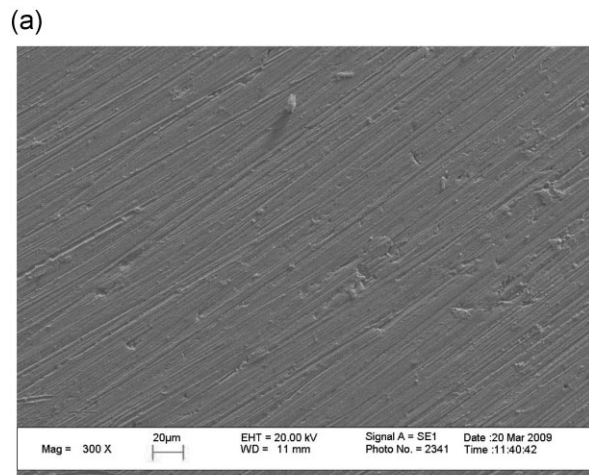
polarization, EIS, and SEM/EDX techniques and the main conclusions are:

(i) A dosage of Na_3PO_4 stimulates the copper corrosion, and the corrosion rate increases with increasing Na_3PO_4 concentration, whereas the mixture of BTA and Na_3PO_4 shows good inhibition for copper in aqueous TBAB solution.

(ii) The inhibition action of the mixture of BTA and Na_3PO_4 on the corrosion of copper is mainly due to the inhibition of the anodic process of corrosion. The IE of a mixture consisting of 2 g/L BTA and 1 g/L Na_3PO_4 was about 96%.

(iii) The mixture of BTA and Na_3PO_4 inhibits the corrosion of copper better than BTA by itself, indicating that Na_3PO_4 has a synergistic role with BTA on the corrosion inhibition of copper in TBAB aqueous solution. EDX analysis has revealed the presence of P and N on the copper surface formed in 17 wt% TBAB solution containing inhibitor mixture, probably indicating incorporation of cupric phosphate and BTA into the surface layer formed.

6 References

[1] I. Tanasawa, S. Takao, presented at *Proceedings 4th International Conf. on Gas Hydrates*, Yokohama, Japan, May 19–23 **2002**, pp. 963–967.

[2] R. Xiao, S. S. Wu, L. G. Tang, C. Huang, Z. P. Feng, presented at *Proc. 10th Inter Conf. on Thermal Energy Storage*, NJ, USA **2006**, pp. 89–96.

[3] H. Oyama, W. Shimada, T. Ebinuma, Y. Kamata, S. Takeya, T. Uchida, J. Nagao, H. Narita, *Fluid Phase Equilibr.* **2005**, *234*, 131.

[4] W. Shimada, T. Ebinuma, H. Oyama, Y. Kamata, H. Narita, *J. Cryst. Growth* **2005**, *274*, 246.

[5] W. Shimada, T. Ebinuma, H. Oyama, S. Takeya, T. Uchida, J. Nagao, H. Narita, presented at *Proceedings 4th International Conf. on Gas Hydrates*, Yokohama, Japan, May 19–23 **2002**, pp. 557–560.

[6] S. Liu, N. N. Xu, J. M. Duan, Z. Zeng, Z. P. Feng, R. Xiao, *Corros. Sci.* **2009**, *51*, 1356.

[7] S. Liu, Y. Zhong, R. Y. Jiang, Z. Zeng, Z. P. Feng, R. Xiao, *Corros. Sci.* **2011**, *53*, 746.

[8] S. Liu, J. M. Duan, R. Y. Jiang, Z. P. Feng, R. Xiao, *Mater. Corros.* **2011**, *62*, 47.

[9] I. Dugdale, J. B. Cotton, *Corros. Sci.* **1963**, *3*, 69.

[10] F. Mansfeld, T. Smith, E. P. Parry, *Corrosion* **1971**, *27*, 289.

[11] D. Thierry, C. Leygraf, *J. Electrochem. Soc.* **1985**, *132*, 1009.

[12] D. Tromans, R. H. Sun, *J. Electrochem. Soc.* **1991**, *138*, 3235.

[13] A. D. Modestov, G. D. Zhou, Y. P. Wu, T. Notoya, D. P. Schweinsberg, *Corros. Sci.* **1994**, *36*, 1931.

[14] L. Tommesani, G. Brunoro, A. Frignani, C. Monticelli, M. Dalcolle, *Corros. Sci.* **1997**, *39*, 1221.

[15] J. H. Chen, Z. C. Lin, S. Chen, L. H. Nie, S. Z. Yao, *Electrochim. Acta* **1998**, *43*, 265.

[16] A. M. Fenelon, C. B. Breslin, *J. Appl. Electrochem.* **2001**, *31*, 509.

[17] T. Kosec, I. Milošev, B. Pihlar, *Appl. Surf. Sci.* **2007**, *253*, 8863.

[18] M. Finšgar, A. Lesar, A. Kokalj, I. Milošev, *Electrochim. Acta* **2008**, *53*, 8287.

[19] F. M. Bayoumi, A. M. Abdullah, B. Attia, *Mater. Corros.* **2008**, *59*, 691.

[20] T. Kosec, D. K. Merl, I. Milošev, *Corros. Sci.* **2008**, *50*, 1987.

[21] H. Hassairi, L. Bousselmi, S. Khosrof, E. Triki, *Mater. Corros.* **2008**, *59*, 32.

[22] G. Lewis, *Br. Corros. J.* **1981**, *16*, 169.

[23] M. M. Musiani, G. Mengoli, *J. Electroanal. Chem.* **1987**, *217*, 187.

[24] P. G. Cao, J. L. Yao, J. W. Zheng, R. A. Gu, Z. Q. Tian, *Langmuir* **2002**, *18*, 100.

[25] S. M. Milić, M. M. Antonijević, *Corros. Sci.* **2009**, *51*, 28.

[26] M. M. Huković, R. Babić, A. Marinović, *J. Electrochem. Soc.* **1998**, *145*, 4045.

[27] V. Brusic, M. A. Frisch, B. N. Eldridge, F. P. Novak, F. B. Kaufman, B. M. Rush, G. S. Frankel, *J. Electrochem. Soc.* **1991**, *138*, 2253.

[28] D. Q. Zhang, L. X. Gao, G. D. Zhou, *Corros. Sci.* **2004**, *46*, 3031.

[29] D. M. Bastidas, *Surf. Interface Anal.* **2006**, *38*, 1146.

[30] E. Otero, J. M. Bastidas, *Mater. Corros.* **1996**, *47*, 133.

[31] M. Attarchi, M. S. Roshan, S. Norouzi, S. K. Sadrnezhaad, A. Jafari, *J. Electroanal. Chem.* **2009**, *633*, 240.

[32] M. Finšgar, I. Milošev, *Mater. Corros.* **2011**, *62*, 956.

[33] N. Souissi, L. Bousselmi, S. Khosrof, E. Triki, *Mater. Corros.* **2003**, *54*, 318.

[34] N. Souissi, E. Triki, *J. Mater. Sci.* **2007**, *42*, 3259.

[35] N. Souissi, E. Triki, *Corros. Sci.* **2008**, *50*, 231.

[36] B. R. Lewandowski, D. A. Lytle, J. C. Garno, *Langmuir* **2010**, *26*, 14671.

[37] S. O. Pehkonen, A. Palit, X. Zhang, *Corrosion* **2002**, *58*, 156.

[38] Y. Zhe, S. O. Pehkonen, *Water Sci. Technol.* **2004**, *49*, 73.

[39] S. Reiber, *J. Am. Water Works Assoc.* **1989**, *81*, 114.

[40] D. M. Dodrill, M. Edwards, *J. Am. Water Works Assoc.* **1995**, *87*, 74.

[41] M. Edwards, L. Hidmi, D. Gladwell, *Corros. Sci.* **2002**, *44*, 1057.

[42] J. Dartmann, T. Alex, T. Dorsch, E. Schevalje, K. Johannsen, *Acta Hydrochim. Hydrobiol.* **2004**, *32*, 25.

[43] B. D. Chambers, S. R. Taylor, *Corros. Sci.* **2007**, *49*, 1597.

[44] L. Niu, C. N. Cao, H. C. Lin, G. L. Song, *Corros. Sci.* **1998**, *40*, 1109.

[45] N. Attarzadeh, K. Raeissi, M. A. Golozar, *Prog. Org. Coat.* **2008**, *63*, 167.

[46] E. A. Aba El Meguid, N. K. Awad, *Corros. Sci.* **2009**, *51*, 1134.

[47] Z. Shi, M. Liu, A. Atrens, *Corros. Sci.* **2010**, *52*, 579.

[48] E. Poorqasemi, O. Abootalebi, M. Peikari, F. Haqdar, *Corros. Sci.* **2009**, *51*, 1043.

[49] B. Jabeera, S. M. Shibi, T. S. Anirudhan, *Appl. Surf. Sci.* **2006**, *252*, 3520.

[50] U. Rammelt, S. Koehler, G. Reinhard, *Corros. Sci.* **2008**, *50*, 1659.